International Journal of Autonomous Robotics and Intelligent Systems
Vol. 2, No. 1, June 2026 [17-29]

Comparative Structural Assessment of Shell-Only, Simple Ribs, Honeycomb Core and Full-Solid Composite UAV Wings

Muhammad Afnan Nazmy[1*], Prof. Ir. Ts. Dr. Hazry Bin Hj. Desa[2] and Dr. Azmat Saeed[3]

[1]Faculty of Electrical Engineering & Technology, Universiti Malaysia Perlis, 02600, Arau, Perlis, Malaysia
[2]Centre of Excellence for Unmanned Aerial Systems (COE-UAS), Universiti Malaysia Perlis, 02600, Arau, Perlis, Malaysia
[3]Department of Electrical Engineering, College of E&ME National University of Sciences & Technology (NUST) Islamabad, Pakistan

Received 4 November 2025, Revised 21 January 2026, Accepted 5 May 2026

ABSTRACT

This paper reports a finite-element-analysis (FEA)–driven redesign of a fixed-wing UAV to improve stiffness-to-weight and ultimate strength using composite structures. Four internal architectures sharing an identical outer mold line are compared: (1) full-solid, (2) shell-only (no internal fill), (3) simple ribs, and (4) honeycomb core. Using orthotropic laminate models, static and modal analyses are conducted under limit (2.5g) and ultimate (1.5×) load cases with a clamped root boundary. Results show the honeycomb core achieves the best overall structural performance at mid-weight, while the simple ribs concept provides most of the stiffness gains with minimal mass penalty. The shell-only configuration is lightest but too flexible, meanwhile the full-solid is overweight for the constant MTOW. The study provides a reproducible FEA workflow and quantitative metrics (EI, GJ, f_1, safety factor and tip deflection) for UAV teams transitioning away from monolithic wings.

Keywords: Wings Design, UAV, Composite Structures, FEA, Optimization, Weight Reduction

1. INTRODUCTION

Unmanned aerial vehicles (UAVs) increasingly support long-range mapping, inspection and logistics missions that demand high endurance, gust robustness and adequate aeroelastic margins. Wing structural efficiency is critical because it governs empty weight, payload fraction and the stiffness-to-mass balance that controls deflection and aeroelastic safety. Aircraft-structures theory links bending stiffness, *EI* and torsional stiffness, *GJ* to global response, while composite design guidance highlights the importance of laminate architecture and joint integrity [1][2]. Monolithic ("full-solid") wings are simple to fabricate but are typically mass-inefficient, whereas rib-stiffened shells and sandwich torsion boxes can achieve high stiffness at low mass when skins, cores and bonded interfaces are properly engineered [1][2][3][4].

This study isolates structural effects by fixing the outer-mold line (OML) and varying only the internal architecture. A constant MTOW of 10.50 kg anchored to the supplied shell-only baseline is enforced to enable direct payload-margin comparisons. The finite-element-analysis (FEA) workflow captures orthotropic lamina behavior, sandwich-core shear response and mesh verification using standardized property pathways consistent with current practice [2][5][6][7][8]. We report decision-oriented metrics *EI*, *GJ*, f_1, ultimate safety factor, 2.5 g tip

*afnan.hailmy@gmail.com

deflection, and payload impact to compare four architectures (full-solid, shell-only, simple ribs and honeycomb core) under identical OML and load cases.

1.1 Summary of Previous Works

Authoritative texts and handbooks summarize how *EI*, *GJ*, modal characteristics and aeroelastic margins relate, and they document common failure modes in composite skins, cores, and bonded joints [1][2]. Standardized sandwich test methods (ASTM C393/C273/D7249/D7250) provide repeatable procedures to obtain facesheet /core properties, infer sandwich bending and shear stiffness, and support model calibration, while also highlighting sensitivities to bond quality, inserts and local core crushing near load introduction regions [5][6][7][8]. Beyond structural performance, manufacturing cost and production constraints can also affect the practicality of advanced composite concepts [9].

In small-UAV wings, two lightweight structural families are widely used. Rib-stiffened shells (simple ribs) improve stiffness efficiently through spar caps, periodic ribs and shear-web load paths, and they typically remain compatible with lower tooling and more practical field repairs than closed-core sandwich structures [3][10][11]. Sandwich torsion boxes using honeycomb (or foam) cores can achieve higher *GJ* for similar mass, increase f_1 and improve aeroelastic robustness. Studies on stiffness-driven flutter behavior and aeroelastic optimization consistently stress the importance of torsional stiffness distribution in composite wings [3][12][13][14]. Topology- and reliability-guided research further suggests that concentrating material in the torsion box can produce large stiffness gains with modest mass penalties, motivating decision-oriented architecture comparisons [10][15][16].

Despite progress, cross-comparison is often difficult because studies commonly vary geometry, mission assumptions or constraints, reducing transferability. Experimental work using static whiffletree loading and modal tests shows that physical validation is valuable to quantify manufacturing effects and calibrate FEA assumptions for composite UAV wings [11][17]. Therefore, a controlled FEA comparison that holds OML, load cases and MTOW constant, while reporting a unified metric set (*EI*, *GJ*, f_1, tip deflection, ultimate safety factor and payload margin), remains useful when grounded in current standards and composite practice [2][4][5][6][7][8].

1.2 Baseline for Shell-Only Configuration

Table 1 summarizes the supplied shell-only baseline that anchors our FEA and comparisons. These data fix the structural targets bending stiffness *EI*, torsional stiffness *GJ*, first bending mode f_1 and ultimate load capacities consistent with standard aircraft structures practice and composite design guidance [1][2]. The procedures used to determine and validate sandwich stiffness and core / skin properties (and to calibrate FE models) follow established ASTM methods for beam flexure and core shear [5][6][7][8]. From the total empty weight of 6.50 kg and both-wings mass of 2.62 kg, a constant non-wing empty mass of 3.88 kg was inferred, and combined with the useful 4.00 kg load, this yields a common MTOW of 10.50 kg used for all variants. The same load cases (2.5 g limit with a 1.5× ultimate factor) are applied to each internal architecture, enabling an apples-to-apples assessment of strength, stiffness, and payload margin; inclusion of f_1 reflects its role in aeroelastic safety screening [1][2][12].

Table 1 Supplied shell-only metrics used to anchor the study and derive constant non-wing masses

Metric / Test Condition	Baseline Value
Ultimate tensile load capacity (shell)	2.8 kN
Ultimate bending load (wing spar)	1.9 kN·m
Safety factor (structural margin)	1.35
Wing bending stiffness (EI)	420 N·m^2
Torsional stiffness (GJ)	185 N·m^2
Modal frequency (first bending mode)	22 Hz
Wing assembly weight (per wing)	1.31 kg
Both wings weight	2.62 kg
Empennage weight	0.85 kg
Total empty weight	6.50 kg
Payload capacity (useful load)	4.0 kg

2. MATERIAL AND METHODS

The details of the modeling and evaluation workflow used to compare four internal wing architectures under an identical outer-mold line are discussed. To ensure comparable results, all analyses are performed in SI units with a fixed MTOW of 10.50 kg and common load cases (2.5 g limit, 1.5× ultimate). The geometry and configurations (Section 2.1) and the orthotropic material models and layups (Section 2.2) were first defined. The finite-element discretization, element types, meshing strategy and convergence targets are described in Section 2.3. Boundary conditions and applied aerodynamic / torsional loads used to extract global stiffness and modal properties are specified in Section 2.4. Finally, Section 2.5 states the failure criteria and the post-processing metrics reported bending stiffness EI, torsional stiffness GJ, first bending mode f_1, safety factor at ultimate and tip deflection at 2.5 g.

2.1 Geometry and Configurations

A single outer-mold line (OML) was modeled in CATIA V5 and held fixed to isolate the effect of internal structure. The shell-only configuration is thin carbon-composite skins with no interior fill and minimal spar caps serve as the baseline for mass and load normalization in the FEA. Against this baseline, full-solid (monolithic, polymer-rich as-built), simple ribs (periodic glass / CF ribs at 80–100 mm with a central shear web and UD cap strips) and honeycomb core (continuous 10 mm Nomex torsion box from 20–60 % chord with carbon skins) were evaluated. Figures 1 to 4 show the common OML and the internal layouts for full-solid, shell-only baseline, simple ribs and honeycomb core respectively.

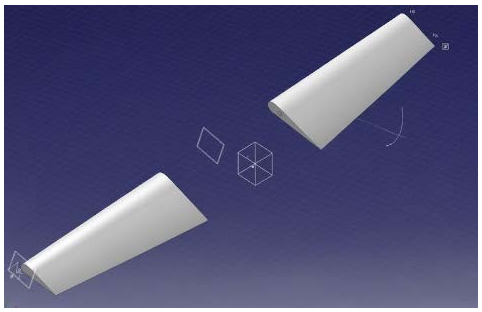

Figure 1. Full-solid monolithic model

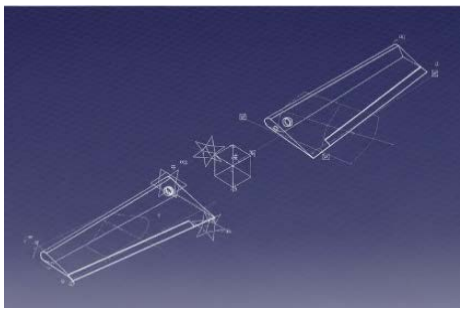

Figure 2. Shell-only

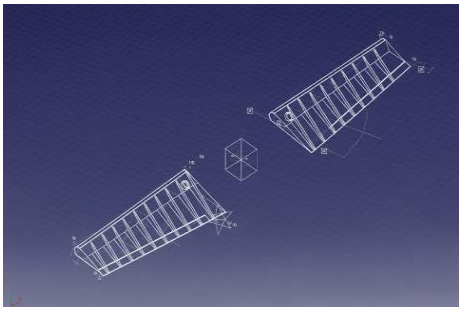

Figure 3. Simple ribs model

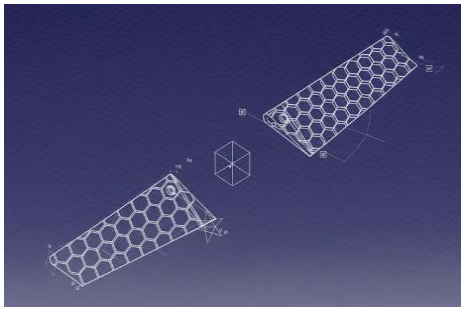

Figure 4. Honeycomb core model

2.2 Material Models

The orthotropic lamina properties were used for carbon plies as shown in Figure 5 (representative values: $E_1 \approx 135$ GPa, $E_2 \approx 10$ GPa, $G_{12} \approx 5$ GPa, $\nu_{12} \approx 0.3$, $\rho \approx 1600$ kg·m^{-3}). Core materials were modeled as low-density honeycomb / foam ($\rho \approx 29$–60 kg·m^{-3}) with appropriate shear moduli. Layups for skins typically followed (45° / 0° / 90° / 0° / −45°) to balance stiffness and strength, while UD cap strips aligned with the spanwise axis to carry bending.

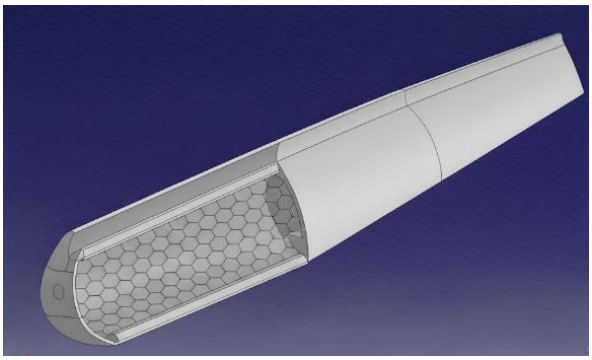

Figure 5. Carbon piles

Aerospace-grade orthotropic CFRP laminates with symmetric, balanced stacking are used across all configurations to preclude coupling effects. The honeycomb architecture is modeled as a sandwich structure with a 10 mm core resisting transverse shear, while the simple-ribs concept employs thin bonded composite webs. Interfaces utilize tie constraints to simulate perfect bonding, representing an ideal manufacturing baseline. Tie constraints represent an idealized upper-bound interface condition (perfect adhesion and no progressive debonding). Therefore, interface-driven failures such as adhesive debonding, bond line voids and skin–core delamination are not captured in the present simulations. As a result, the reported safety factors should be interpreted as optimistic with respect to bond defects. This modeling choice is intended to provide a consistent baseline comparison of internal architectures under identical geometry and load definitions, while interface degradation is addressed in the validation plan via bond integrity quantification. Structural integrity is evaluated using the Tsai-Wu criterion for plies and maximum allowable limits for core shear. Table 2 summarizes the material and layup used.

Table 2 Material and layup summary used for FEA (representative baseline)

Part	Material / Model	Layup (representative)	Key Notes
Skins (all concepts)	CFRP orthotropic laminate	45° / 0° / −45° / 90°	Symmetric / balanced; angles limited to 0°, ±45°, 90°
Spar caps (if used)	CFRP orthotropic (0° dominated)	0° / 0° / ±45° / 0°	0° carries bending; ±45° for shear transfer
Ribs (simple ribs)	CFRP orthotropic laminate	±45° / 0° / 90°	Web stiffeners; bonded to skins
Core (honeycomb)	Equivalent orthotropic core	tc=10 mm	Core carries shear; skins carry bending
Interfaces	Tie / perfect bond	-	Skin–rib and skin–core assumed perfectly bonded
Failure checks	Tsai–Wu (plies) + core shear	-	Used for safety factor / constraint evaluation

2.2.1 Finite-Element Discretization

Skins, cores and spars were modeled using shell, solid orthotropic and beam elements, respectively. Confirmed by an h-refinement study targeting <3% tip deflection variance at 2.5g, the mesh utilizes 6–10 mm elements over the torsion box and 12–18 mm elsewhere, with specific refinement at the root and load points, as shown in Figure 6.

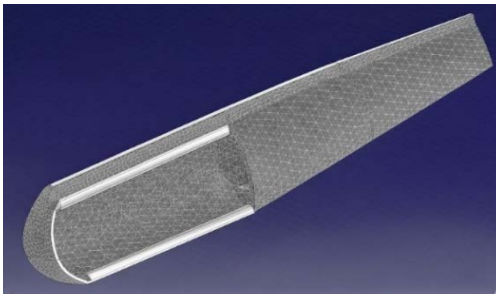

Figure 6. Shell elements modeled

2.3 Boundary Conditions and Loads

A clamped root boundary was applied. Load cases included elliptic spanwise lift scaled to the 2.5g limit and a torsional moment about the elastic axis to evaluate GJ. Analysis comprised modal extraction of the first bending mode, f_1 and ultimate strength verification at 1.5× limit loads, as shown in Figure 7.

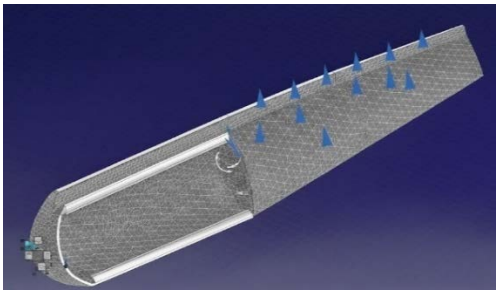

Figure 7. Distributed aerodynamic lift analysis

2.3.1 Failure Criteria and Post-Processing

Lamina stresses were evaluated with a Tsai-Wu failure index for composite skins, where the maximum shear was tracked in cores and webs. Global metrics were computed as follows: EI and GJ from load–deflection and load–twist slopes, f_1 from Lanczos extraction, safety factor as the ratio between ultimate capacity and demanded ultimate load, and tip deflection measured at the semi-span tip under 2.5g, as shown in Figure 8.

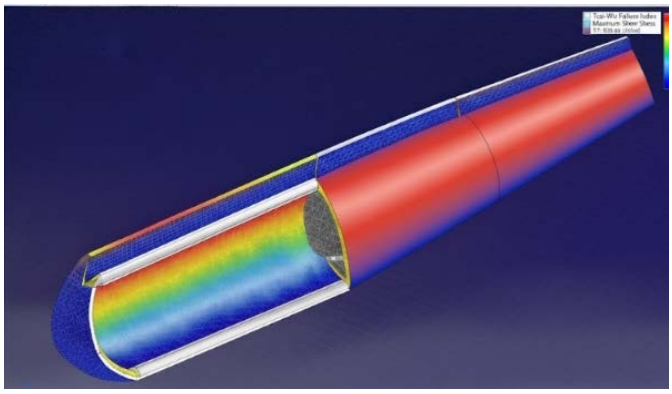

Figure 8. Lamina stresses evaluation

3. RESULTS AND DISCUSSION

3.1 Operational System

Tables 3 to 5 show the collected data for full-solid (monolithic), simple ribs (periodic ribs + spar caps) and honeycomb core (continuous torsion box). They also show the value for metric or test condition for ultimate tensile load capacity (shell), ultimate bending load (wing spar), safety factor (structural margin), wing bending stiffness (EI), torsional stiffness (GJ), modal frequency (first bending mode), wing assembly weight (per wing), both wings weight, empennage weight, total empty weight and payload capacity (useful load).

Table 3 Full-solid (monolithic)

Metric / test condition	Value
Ultimate tensile load capacity (shell)	3.2 kN
Ultimate bending load (wing spar)	2.5 kN·m
Safety factor (structural margin)	1.55
Wing bending stiffness (EI)	680 N·m^2
Torsional stiffness (GJ)	260 N·m^2
Modal frequency (first bending mode)	27 Hz
Wing assembly weight (per wing)	3.93 kg
Both wings weight	7.86 kg
Empennage weight	0.85 kg
Total empty weight	11.74 kg
Payload capacity (useful load)	-1.24 kg (overweight)

Table 4 Simple ribs (periodic ribs + spar caps)

Metric / Test Condition	Value
Ultimate tensile load capacity (Shell)	3.6 kN
Ultimate bending load (wing spar)	2.9 kN·m
Safety factor (structural margin)	1.75
Wing bending stiffness (EI)	950 N·m^2
Torsional stiffness (GJ)	360 N·m^2
Modal frequency (first bending mode)	31 Hz
Wing assembly weight (per wing)	1.55 kg
Both wings weight	3.10 kg
Empennage weight	0.85 kg
Total empty weight	6.98 kg
Payload capacity (useful load)	3.52 kg

Table 5 Honeycomb core (continuous torsion box)

Metric / Test Condition	Value
Ultimate tensile load capacity (shell)	4.6 kN
Ultimate bending load (wing spar)	3.8 kN·m
Safety factor (structural margin)	2.10
Wing bending stiffness (EI)	1,250 N·m^2
Torsional stiffness (GJ)	510 N·m^2
Modal frequency (first bending mode)	36 Hz
Wing assembly weight (per wing)	1.70 kg
Both wings weight	3.40 kg
Empennage weight	0.85 kg
Total empty weight	7.28 kg
Payload capacity (useful load)	3.22 kg

3.2 Architecture-Level Comparison

Table 6 summarizes mass, stiffness, modal and strength metrics for the four architectures under a fixed MTOW of 10.5 kg. Empty weight equals non-wing mass (3.88 kg from the shell-only baseline) plus the two-wing mass for each concept, whereas payload is MTOW minus empty weight.

Table 6 Summarized mass, stiffness, modal and strength metrics (four architectures)

Configuration	Full-solid	Shell-only (no fill)	Simple ribs	Honeycomb core
Wing mass per wing (kg)	3.93	1.31	1.55	1.70
Both wings (kg)	7.86	2.62	3.10	3.40
Empty weight (kg)	11.74	6.50	6.98	7.28
Payload (kg)	-1.24 (overweight)	4.00	3.52	3.22
EI (N·m^2)	680	420	950	1250
GJ (N·m^2)	260	185	360	510
f_1 (Hz)	27	22	31	36
Ultimate bending (kN·m)	2.5	1.9	2.9	3.8
Ultimate tensile (kN)	3.2	2.8	3.6	4.6
Safety factor	1.55	1.35	1.75	2.10
Tip deflection @ 2.5 g (mm)	24	31	21	15

From the results, it can be summarized that the full-solid wing leaves no payload margin under the constant MTOW. Meanwhile, the shell-only configuration is light but exhibits the lowest EI, GJ, and f_1. On the other hand, simple ribs achieve large stiffness gains (+105% GJ vs. shell-only) for only +0.48 kg additional mass (both wings) and honeycomb core provides the best overall performance with $EI \approx 1.25\times10^3$ N·m^2 and $GJ \approx 5.1\times10^2$ N·m^2 at a modest mass increase.

Figures 9 to 15 summarize the comparative performance of the four wing architectures under a fixed MTOW of 10.5 kg and common 2.5 g / 1.5× load cases. The charts report both-wing mass, empty weight, payload, bending stiffness (EI), torsional stiffness (GJ), first bending mode (f_1), and tip deflection. As shown, the honeycomb core delivers the strongest overall structural / aeroelastic response with modest mass growth, while simple ribs offer the best stiffness-to-cost trade. Meanwhile, shell-only is lightest but overly compliant, and full-solid is robust yet operationally overweight.

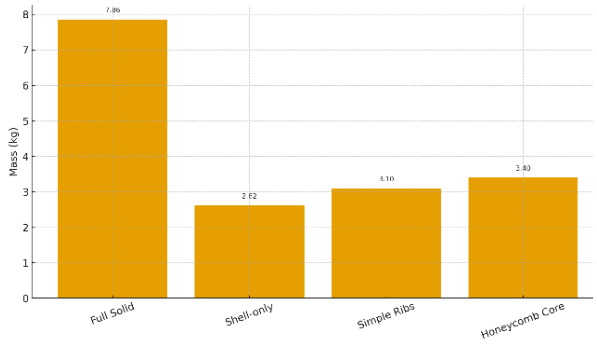

Figure 9. Both wings mass by configuration

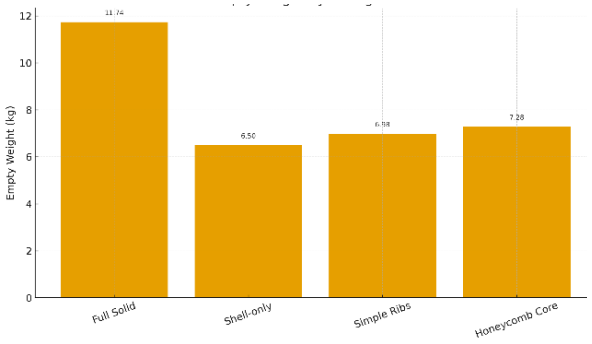

Figure 10. Empty weight by configuration

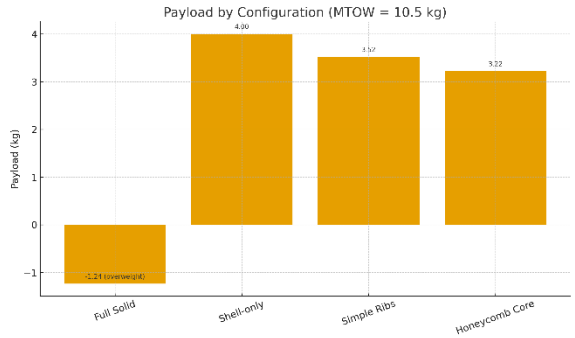

Figure 11. Payload by configuration (MTOW= 10.5 kg)

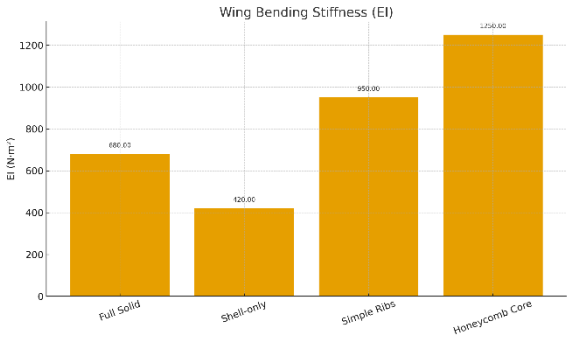

Figure 12. Wing bending stiffness (EI)

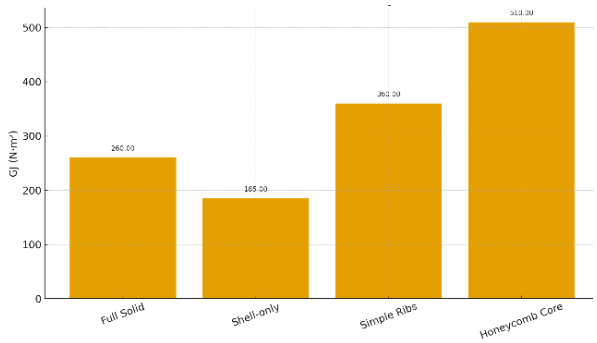

Figure 13. Torsional stiffness (GJ)

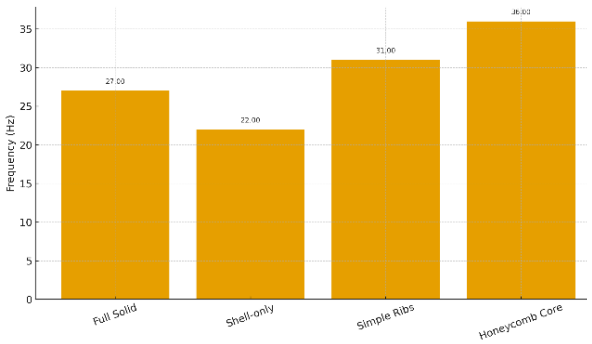

Figure 14. First Bending Mode (f_1)

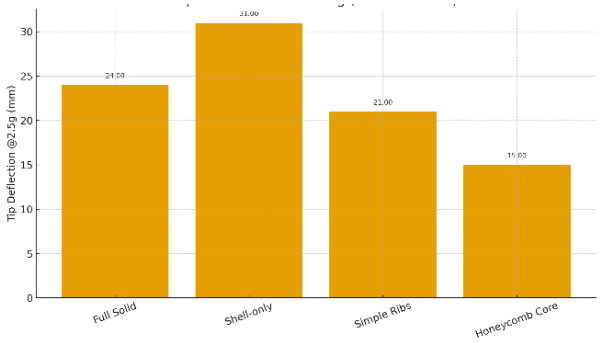

Figure 15. Tip deflection under 2.5g

Under a 2.5g limit loading, predicted wingtip deflections were 24 mm (full-solid), 31 mm (shell-only), 21 mm (simple sibs) and 15 mm (honeycomb). Ultimate checks (1.5× factor) yielded safety factors consistent with laminate and core allowable: ≈ 1.35 for shell-only, 1.75 for simple ribs and ≥2.10 for honeycomb. The higher GJ of ribbed / honeycomb concepts improves aileron effectiveness and flutter margins by limiting torsional compliance.

3.3 Deflection, Strain and Safety

By using the triangular load bending deflection formula with the EI values as in Equation (1), deflection is determined. It is then converted to mm and compared to the reported δ_{total}:

$$\delta_b = \frac{W\,L^3}{15\,EI} \text{ (in meters)} \tag{1}$$

For the same triangular load, with root surface strain at 2.5 g, the root curvature is as Equation (2):

$$\kappa = M/EI \tag{2}$$

Eliminating M using the deflection relation gives a simple link to deflection as in Equation (3):

$$\varepsilon_{\text{root}} = \kappa\, c = \frac{5\,c}{L^2}\,\delta_{\text{total}} \tag{3}$$

where $c = 0.01$ m, $L = 1.15$ m.

For torsional effectiveness (aileron authority, flutter margin proxy), a simple effectiveness proxy is that twist under a given torque scale with $1/GJ$, relative twist vs. shell-only as in Equation (4):

$$\frac{\theta}{\theta_{\text{Shell}}} \approx \frac{GJ_{\text{Shell}}}{GJ} \tag{4}$$

3.4 Mesh Convergence and Sensitivity or Uncertainty Screening (Material, Tolerance and Loading Variations)

Mesh refinement halved the global element size over the torsion box, changing tip deflection by <2.5% and f_1 by <1.8%, which is within the 3% target. Parameter sweeps indicated that increasing honeycomb core thickness from 10 mm to 12 mm improves EI by ~18% for ~6% mass growth, rib spacing above 100 mm begins to induce local skin wrinkling near the root under compression at 2.5g.

To assess the robustness of the comparative conclusions against real-world variability, a screening sensitivity / uncertainty analysis is performed for key sources of uncertainty in composite UAV wings: (i) laminate stiffness scatter (e.g., face-sheet modulus), (ii) sandwich-core shear variability (for honeycomb-core concept), and (iii) loading uncertainty (e.g., maneuver / gust factor). A one-factor-at-a-time (OFAT) perturbation is used with small representative variations (±10% for stiffness-related properties and ±5% for load scaling). The impact is evaluated on the main decision metrics tip deflection δ, first bending frequency f_1, and safety factor (SF) using normalized sensitivity indices as in Equation (5):

$$S = \frac{\Delta y/y}{\Delta x/x} \tag{5}$$

This screening does not replace full probabilistic analysis; instead, it provides a compact robustness check and indicates which assumptions most strongly influence the reported trends. Table 7 summarizes these.

Table 7 Sensitivity / uncertainty inputs and expected impact on key outputs (screening)

Uncertain input (perturbation)	Applies mainly to	Key affected outputs	Normalized sensitivity (S) (screening)	Interpretation (simple)
Face-sheet laminate stiffness (Eface) (±10%)	All concepts	δ, f_1	Sδ ≈ −1Sf_1 ≈ +0.5	Lower stiffness → higher deflection; higher stiffness → higher f_1
Core shear stiffness (Gcore) (±10%)	Honeycomb-core	δ, sometimes f_1	Sδ≈−1 (when shear-dominated)	Core shear variability strongly affects sandwich deflection
Load scale factor (n) (±5%)	All concepts	δ, SF	Sδ ≈ +1SSF ≈ −1	Higher load increases deflection and reduces safety margin
Strength allowables (σallow) (±10%)	All concepts	SF	SSF ≈ +1	Higher allowables raise SF approximately proportionally
Mass (m) (±5%)	All concepts	f_1	Sf_1 ≈ −0.5	Heavier wing reduces frequency (dynamic margin)

3.5 Discussion

Torsional stiffness (GJ) is frequently the binding constraint for UAV aeroelastic safety and control authority. While continuous honeycomb cores maximize GJ and flutter margins efficiently, they demand rigorous quality assurance (e.g., bond-line integrity, NDT) and complicate field repairs. Conversely, ribbed shells offer a compelling balance of specific stiffness and repair agility with lower tooling costs. Since realized performance hinges on manufacturing fidelity rather than 'paper properties', design selection must weigh idealized metrics (EI, GJ, f_1) against the process sensitivities summarized in Table 8. Ultimately, shell-only variants are economical but compliant, and honeycomb excels in performance, whereas ribbed designs optimize the cost-stiffness trade-off, rendering full-solid options obsolete due to weight.

Table 8 Practical comparison of internal architectures (relative, qualitative)

Architecture	Manufacturability	Relative Cost	Repairability	Robustness to Process / Defects	Main Practical Risk
Full-solid	Low–med (simple cure, high material)	High	Low	High (few bonds)	Overweight → payload penalty
Shell-only	High (simplest build)	Low	Med	Med–low	Excess deflection / buckling risk
Simple ribs	Medium (extra parts + bonding)	Low–Med	High	Med–high	Rib–skin debond / local stress
Honeycomb core	Low (bonding / QC critical)	Med–High	Med–low	Medium	Skin–core debond / core crush, moisture

While structural metrics (EI, GJ, f_1) define performance, practical selection must weigh manufacturing effort, cos, and process sensitivity specifically bond quality. The shell-only configuration is cost-effective but compliant; simple ribs offer high specific stiffness with moderate complexity and good repairability; and honeycomb cores deliver peak performance but demand strict QA and are difficult to repair. Conversely, the full-solid option is robust but operationally impractical due to weight. Consequently, structural rankings must be contextualized by the qualitative cost / complexity screening in Table 9.

Table 9 Relative cost / complexity screening (1 = lowest, 5 = highest)

Architecture	Build complexity	Cost level	QA demand	Repair difficulty	Main driver
Shell-only	1	1	1	2	Lowest parts and bonding
Simple ribs	3	2	3	2	Added ribs + rib–skin bonding
Honeycomb core	5	4	5	4	Skin–core bonding control + QC; core repairs
Full-solid	2	5	2	4	High material volume (weight-driven)

4. CONCLUSION

This paper compared four composite fixed-wing UAV wing internal architectures (full-solid, shell-only, simple ribs, and honeycomb core) under the same outer mold line (OML) and load cases using unified structural metrics (EI, GJ, f_1), safety factor, and tip deflection. The results indicate that the honeycomb-core concept provides the best overall stiffness / deflection performance at moderate mass, while simple ribs offer a strong stiffness-to-weight improvement with lower manufacturing complexity. The shell-only concept is the simplest baseline but is comparatively

compliant, and the full-solid concept is generally impractical under a fixed MTOW due to weight and payload penalties.

However, there are a few limitations, where these conclusions rely on idealized FEA assumptions (nominal properties, perfect bonding), excluding stochastic defects (voids, fatigue) and manufacturing scatter. Consequently, absolute margins may deviate from physical hardware. Future work will calibrate the FE models via static load testing (strain / deflection) and experimental modal analysis (identifying f_1), with specific emphasis on bond integrity quantification to address manufacturing variability in ribbed and honeycomb architectures.

REFERENCES

[1] T. H. G. Megson, 2021. Aircraft Structures for Engineering Students, Elsevier, doi: 10.1016/C2019-0-03113-5.

[2] SAE International, 2025. Composite Materials Handbook (CMH-17), Volume 3, Revision H: Polymer Matrix Composites Materials Usage, Design, and Analysis.

[3] A. Kausar, I. Ahmad, S. A. Rakha, M. H. Elsa, A. Diallo, 2023. State-of-the-art of sandwich composite structures: Manufacturing-to-high performance applications, Journal of Composites Science, 7(3):102, 2023, doi: 10.3390/jcs7030102.

[4] B. Castanié, C. Bouvet, M. Ginot, 2020. Review of composite sandwich structure in aeronautic applications, Composites Part C: Open Access, 1, 2020, 100004, doi: 10.1016/j.jcomc.2020.100004.

[5] ASTM International, 2020. ASTM C393/C393M-20, Standard Test Method for Core Shear Properties of Sandwich Constructions by Beam Flexure, doi: 10.1520/C0393_C0393M-20.

[6] ASTM International, 2020. ASTM C273/C273M-20, Standard Test Method for Shear Properties of Sandwich Core Materials, doi: 10.1520/C0273_C0273M-20.

[7] ASTM International, 2020. ASTM D7249/D7249M-20, Standard Test Method for Facesheet Properties of Sandwich Constructions by Long Beam Flexure, doi: 10.1520/D7249_D7249M-20.

[8] ASTM International, 2020. ASTM D7250/D7250M-20, Standard Practice for Determining Sandwich Beam Flexural and Shear Stiffness, doi: 10.1520/D7250_D7250M-20.

[9] L. Morse, L. Cartabia, V. Mallardo, 2022. Reliability-based bottom-up manufacturing cost optimisation for composite aircraft structures, Structural and Multidisciplinary Optimization, 65:159, 2022, doi: 10.1007/s00158-022-03250-9.

[10] S. Sleesongsom, A. I. Kattan, M. Arafa, 2023. Multi-objective reliability-based partial topology optimization of a composite aircraft wing, Symmetry, 15(1):25, doi: 10.3390/sym15010025.

[11] A. Marta, F. A. Wandono, A. Nurrohmad, R. Ardiansyah, I. B. Wiranto, I. R. Alfikri, A. R. Prabowo, G. Nugroho, 2025. Finite element analysis and experimental whiffletree testing of a small UAV composite wing, International Journal of Lightweight Materials and Manufacture, 8, 2025, pp. 483–494, doi: 10.1016/j.ijlmm.2025.07.007.

[12] S. Qiao, J. Jiao, Y. Ni, H. Chen, X. Liu, 2021. Effect of stiffness on flutter of composite wings with high aspect ratio, Mathematical Problems in Engineering, Article 6683032, doi: 10.1155/2021/6683032.

[13] Y. Liu, C. Zhou, J. Shen, A. Ding, 2021. Lightweight design of solar UAV wing structures based on sandwich-equivalent theory, International Journal of Aerospace Engineering, Article 6752410, doi: 10.1155/2021/6752410.

[14] S. Kilimtzidis, V. Kostopoulos, 2023. Static aeroelastic optimization of high-aspect-ratio composite wings via surrogate modelling, Aerospace, 10(3):251, doi: 10.3390/aerospace10030251.

[15] M. S. Sahib, G. Kovács, 2024. Multi-objective optimization of composite sandwich structures using artificial neural networks and genetic algorithm, Results in Engineering, 21, 101937, doi: 10.1016/j.rineng.2024.101937.

[16] S. G. Kontogiannis, 2020. A generalized methodology for multidisciplinary design optimization using surrogate modelling and multifidelity analysis, Optimization and Engineering, doi: 10.1007/s11081-020-09504-z.
[17] M. Milewski, A. Wróbel *et al.*, 2025. Experimental and numerical modal analysis of an unmanned aerial vehicle's composite wing, Simulation Modelling Practice and Theory, 139, 103106, doi: 10.1016/j.simpat.2025.103106.